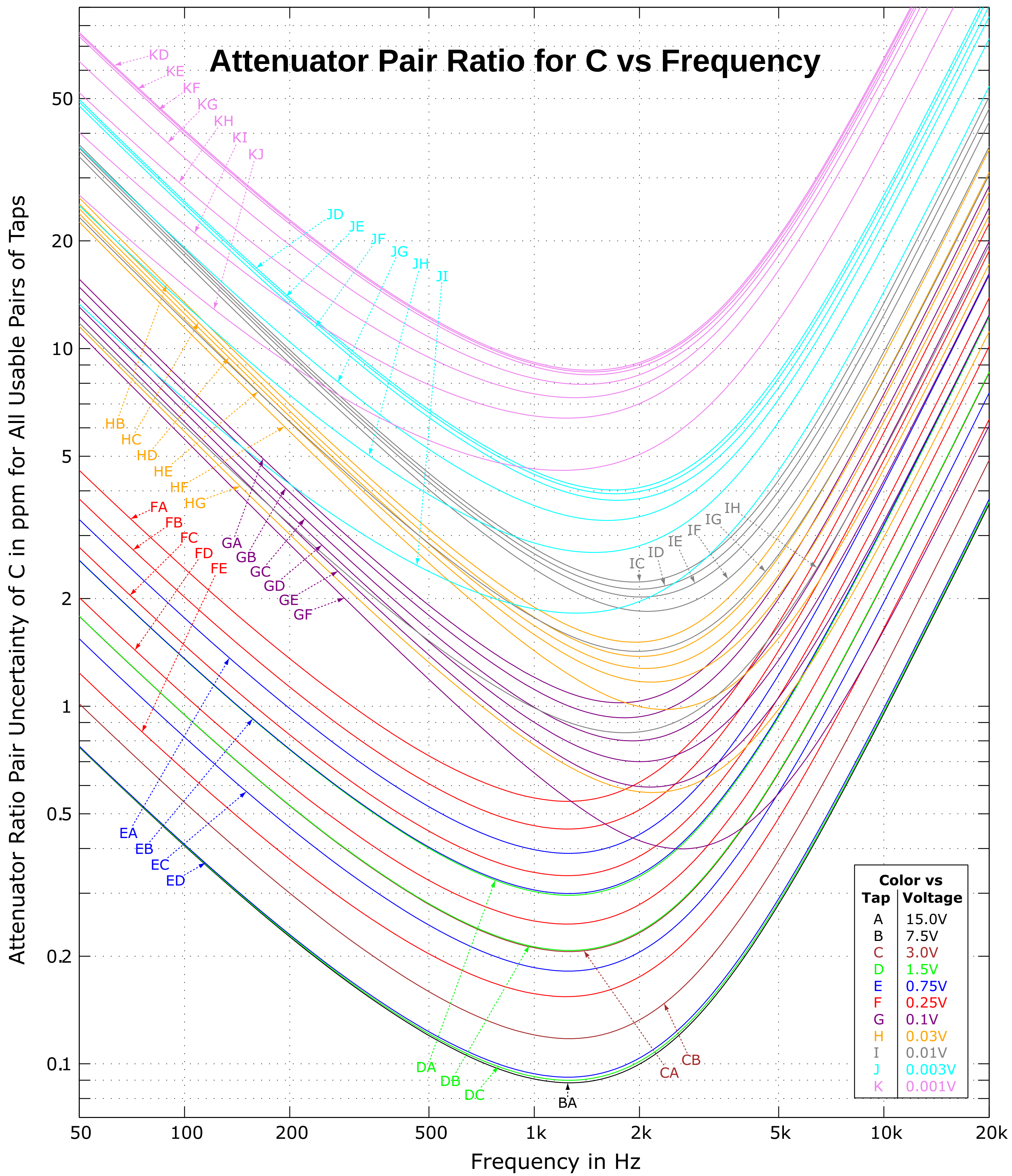

ANDEEN-HAGERLING
31200 Bainbridge Road
Cleveland, Ohio 44139-2231 U.S.A.

Website: www.andeen-hagerling.com
E-mail: info@andeen-hagerling.com
Call: 440-349-0370 Fax: 440-349-0359

2017/08/02

ANDEEN-HAGERLING

AH 2700A Option-E

50 Hz-20 kHz Ultra-precision Capacitance/Loss Bridge

Additional features of the Option-E version of the AH2700A 50Hz-20kHz bridge

The AH2700A Option-E is an enhanced precision version of the basic AH2700A bridge. Much like the AH2500A Option-E, the AH2700A Option-E offers higher precision and significantly enhanced calibration and verification features over its non-Option-E base model. Please refer to the regular AH2700A brochure for a description of basic features.

Features in common with the AH2500A Option-E*

- Quantitatively improved specifications
- Full report of all Internal calibration points
- Real-time temperature corrections
- Selected hardware for higher performance

Features New to the AH2700A Option-E

- Improved hardware to reduce noise and for better thermal performance
- Dynamic Differential Non-Linearity (DDNL) mode
- New specifications for non-linearity and noise
- Attenuator Pair Ratio specification and reporting of the attenuator tap used by each measurement
- Expanded cable and DUT correction commands
- DUT stray capacitance loading correction based on NIST Special Publication 250-76
- User-settable time out-of-calibration warnings
- User-settable temperature out-of-calibration warnings

Verification/Calibration Reports

As part of the Internal verification report, all versions of the AH2700A report the elapsed operating time and temperature difference between the conditions used to obtain the currently stored calibration values and the conditions used to obtain the new verification data. Non-Option-E bridges also report only the one Internal calibration point that is furthest from its nominal value. Option-E bridges produce a more detailed report which includes the status of each of the Internal calibration points in the bridge.

*AH2500A bridges are no longer available.

Real-time Temperature Corrections

An AH2700A Option-E contains additional Internal calibration data in the form of temperature coefficients (TC's) for all Internal calibration points. This TC data is generated when the bridge is manufactured and is considered to be permanent unless the main board or standard capacitor assembly is replaced. The TC data is used to adjust the Internal calibration data so that it is correct for the temperature at which the bridge is operating.

New Noise and DNL Specifications

The resolution and non-linearity uncertainty specifications as defined for the basic AH2700A bridge have been revised for the Option-E version. The resolution specification has been supplemented by two new specifications in the AH2700A Option-E:

1. The first is an Input Noise specification. This is shown graphically on page 11. The units are ppm/$\sqrt{Hz}$ where *Hz* refers to the *measurement rate*, not the test frequency. This new noise specification puts an upper limit on the amount of random noise in the measurements while being independent of DNL performance described next.
2. The second new specification is Differential Non-Linearity (DNL). This specification puts an upper limit on the magnitude of tiny, local steps in the measurement results that occur as a function of capacitance or loss. DNL behaves like the mathematical derivatives of these measurement result functions.

   In all current and previous resolution specifications, this DNL uncertainty and the Input Noise are combined within the resolution specification. In the AH2700A Option-E bridge, the new DNL and noise specs are also specified separately. This can help better understand the effects that limit resolution.

New Integral Non-linearity Specification

In the AH2700A Option-E, a new and different Integral Non-Linearity (INL) specification replaces the non-Option-E AH2700A Non-Linearity spec. This spec uses a commonly accepted method of defining INL as a deviation from a straight line of the transfer curve of the measured value of capacitance (or loss) versus the actual value. Ideally, the lower ends of the transfer curve and the straight line are defined to pass through C=0. In most cases, the upper ends of the curve and the line are defined to pass through the highest capacitance (or loss) reachable by the transformer attenuator tap used to make the current reading. This curve is likely composed of quadratic and higher order curves, all of which are so small that we are unable to quantify their nature. Therefore, we define our INL spec to be within a band whose width has a fixed height centered on the straight line. This width is specified as a function of frequency for capacitance and loss as a set of six equations and two graphs shown later herein. This set gives one INL specification function for each transformer attenuator tap, A through K, as listed in Table 2 on page 3.

When to use DNL versus INL?

DNL uncertainty is important when accurately comparing measurements of two capacitors having closely similar values.

INL uncertainty is important when comparing the sum of the capacitances of two capacitors measured individually against measurements of them taken when connected in parallel. All three measurements must be made on the same attenuator tap.

Dynamic Differential Non-Linearity (DDNL)

This is a new feature which can substantially reduce the magnitude of DNL step flaws in the measured data. It does this by averaging the measured data in regions where these steps are prone to occur. DDNL's availability is dependent on the test frequency and the average time according to Table 1 below. Where possible, DDNL is enabled by default, but can be disabled if desired.

Table 1: Average Times and Frequencies for which DDNL can be Enabled

Average time setting	50-599+ Hz	600-1199+ Hz	1200-4999+ Hz	5000-20000 Hz
<6	Enableable	Inactive	Inactive	Inactive
7	Enableable	Enableable	Inactive	Inactive
8	Enableable	Enableable	Enableable	Inactive
≥9	Enableable	Enableable	Enableable	Enableable

The Attenuator Pair Ratio Uncertainty Spec

Each AH2700A capacitance bridge contains ratio transformers collectively having a set of eleven selectable attenuator taps that allow a variable voltage to be supplied to the H (High) terminal of the bridge. By selecting one of these taps at a time, this voltage can be very precisely set to cover a range from zero to 15 volts thereby allowing the bridge to measure correspondingly larger capacitance values using eleven distinct ranges covering over 100 pF on the A tap range to over 1.65 µF on the K tap range. The A tap range can be calibrated directly by measuring a traceable reference capacitor having a value compatible with this range such as 100 pF. Such direct calibration of the other ten ranges is less desirable due to the limited stability of capacitors having larger values. Inter-comparison of measurements made on adjacent ranges allows all the ranges to be calibrated relative to each other and especially of each to the A tap range. At the same time, uncertainties can be determined for all pairs of ranges (attenuator taps). These uncertainties are used to create the Attenuator Pair Ratio Uncertainty Specifications (APR) for C and D shown as graphs on pages 11 and 12. The non-Option-E AH2700A bridge APR uncertainties are incorporated only into its accuracy specifications.

APR uncertainty is fundamentally different from all the other uncertainties for AH bridges in that APR only applies to a ***pair*** of measurements. It gives an uncertainty based on that pair's not having used the same attenuator tap for both measurements. If the same attenuator tap is used for both members of the pair, then the APR uncertainty is zero.

Application of APR

Suppose your lab has a very stable 100 pF reference capacitor with a high accuracy traceability certificate. Further suppose you have other capacitors having an array of capacitance values. You would like to calibrate these capacitors relative to your traceable 100 pF reference capacitor and you would like to provide a certificate of traceability with these capacitors. Using AH2700A bridges, there are three ways to do this:

1. You can use the AH capacitance calibration procedure described in the AH manual to calibrate your AH2700A non-Option-E bridge. This will allow that bridge to make traceable measurements throughout its range having uncertainties given mainly by the published accuracy specification for that AH2700A. This is a safe way to make traceable measurements, but will not give the tightest possible uncertainties because the AH accuracy specification already allows for a relatively large traceability uncertainty. This traceability uncertainty may be larger than necessary if your traceable 100 pF reference capacitor has a tighter certification.
2. You can apply the same procedure described above but using an AH2700A Option-E bridge. Since the published uncertainties for this bridge will be smaller, you will be able to produce tighter certificates of traceability than with paragraph 1 above.
3. You can use an AH2700A Option-E bridge to accurately measure your traceable 100 pF reference capacitor and record the results (without changing the calibration of your bridge). All subsequent capacitance measurements made with this bridge can then be corrected by the ratio between the earlier recorded results and the traceable certified value of your 100 pF reference capacitor. The uncertainty calculations for these measurements should not include the published accuracy specification for your AH2700A Option-E. Instead, the calculation should include the sum of the traceable uncertainty of your 100 pF reference and the Noise, DNL, and TC for the measurement of your 100 pF reference. In addition, each subsequent capacitance measurement must add the sum of its own Noise, DNL, and TC. A stability uncertainty is not needed unless enough time has passed to justify it. One more uncertainty must be added to this list. This is the Attenuator Pair Ratio (APR) uncertainty. This is needed only for whichever subsequent measurements were made using a different attenuator tap than was used by the measurement of the 100 pF reference capacitor. The attenuator tap used is reported by each measurement result.

Expanded Cable Correction Commands

Correction Models

The cable correction model for the non-Option-E AH2700A allows the user to specify the electrical parameters of the dual coaxial cable that connects the bridge to the DUT. These include the capacitance per meter, inductance per meter, and resistance per meter, as well as the length of the cable. This model does not take into account any frequency dependent behavior of the cable. To make frequency dependent corrections in a non-Option-E bridge, you must specify the cable parameters for each frequency at which a measurement is to be taken.

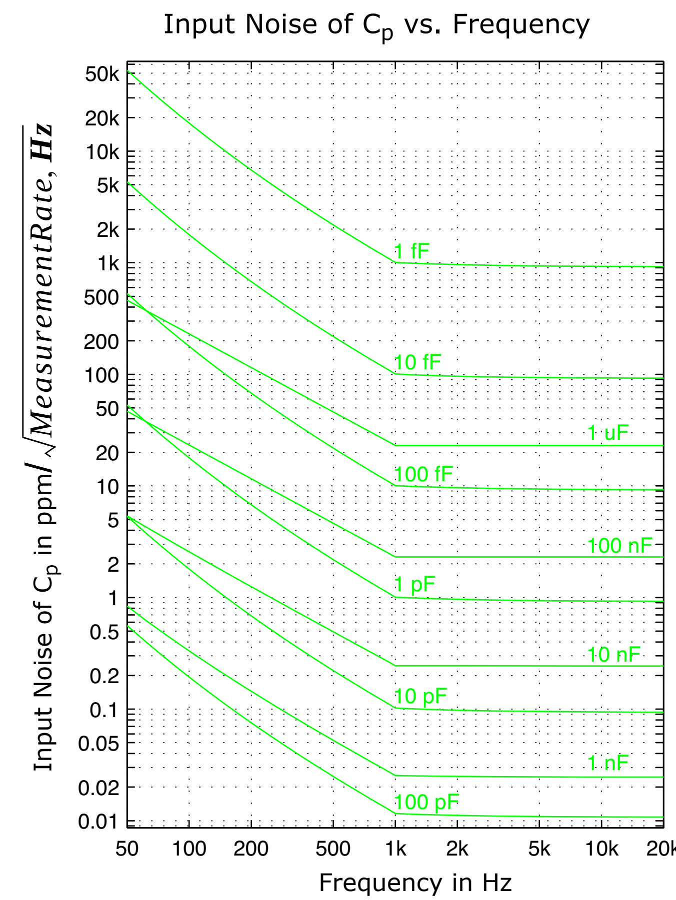

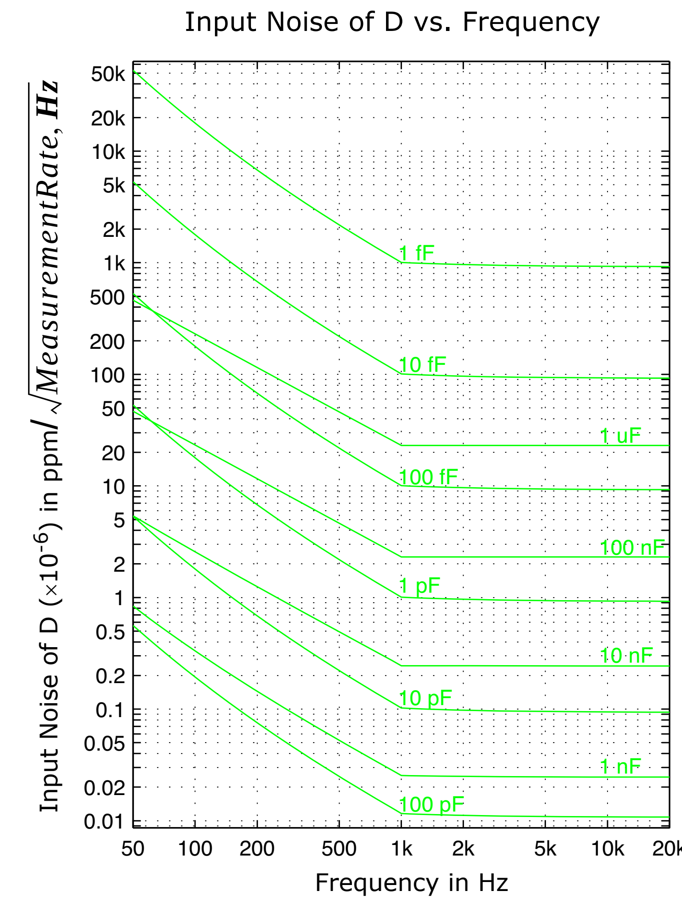

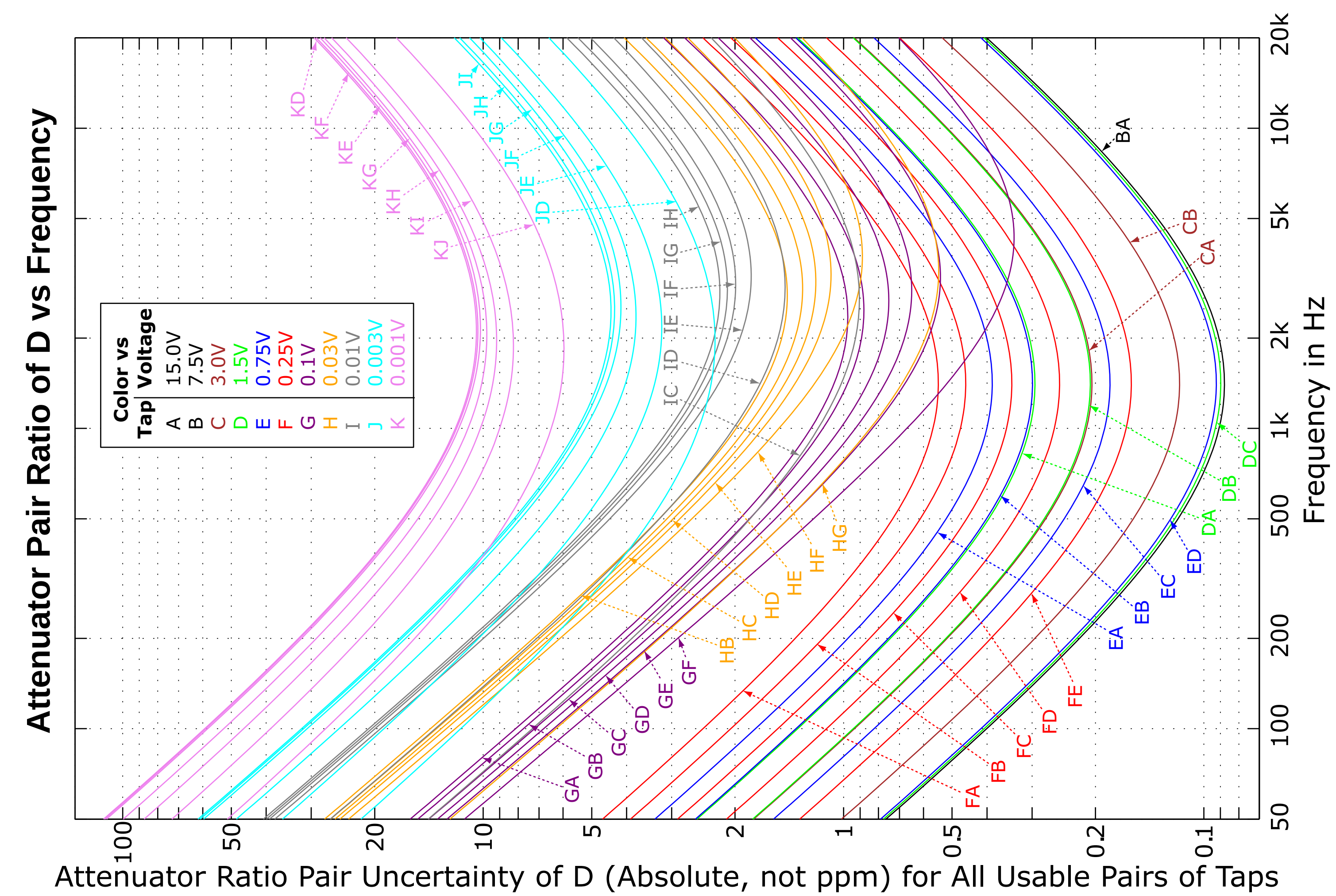

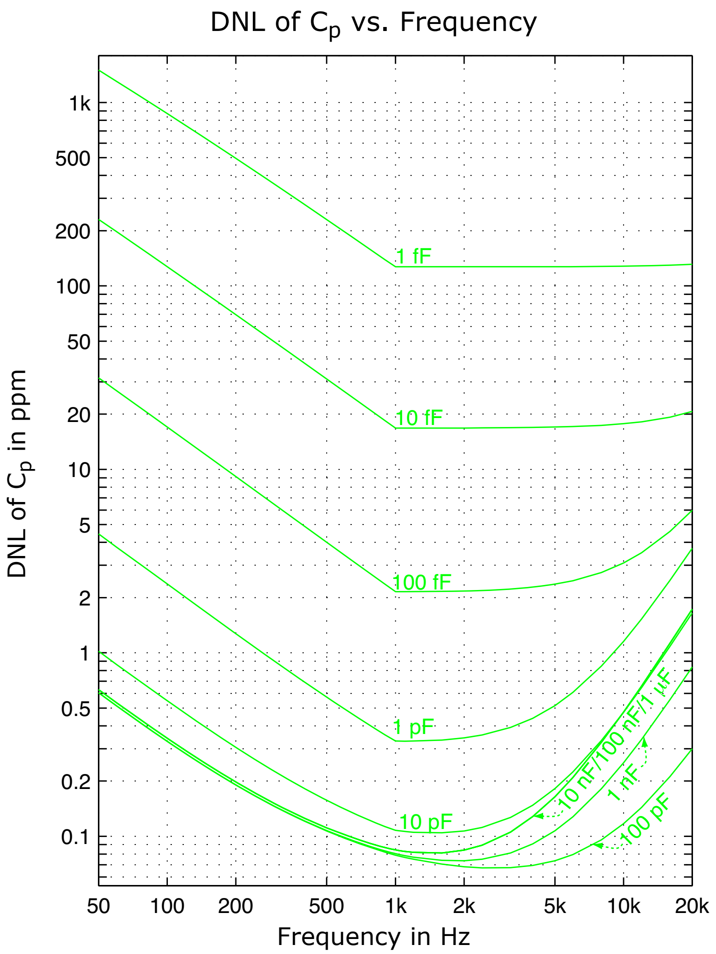

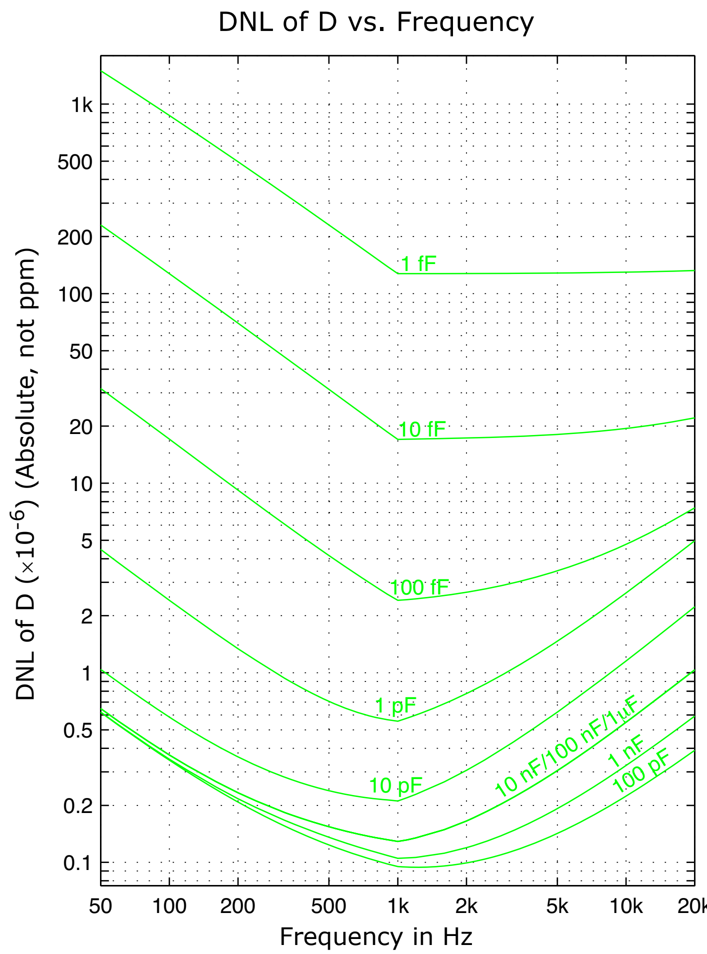

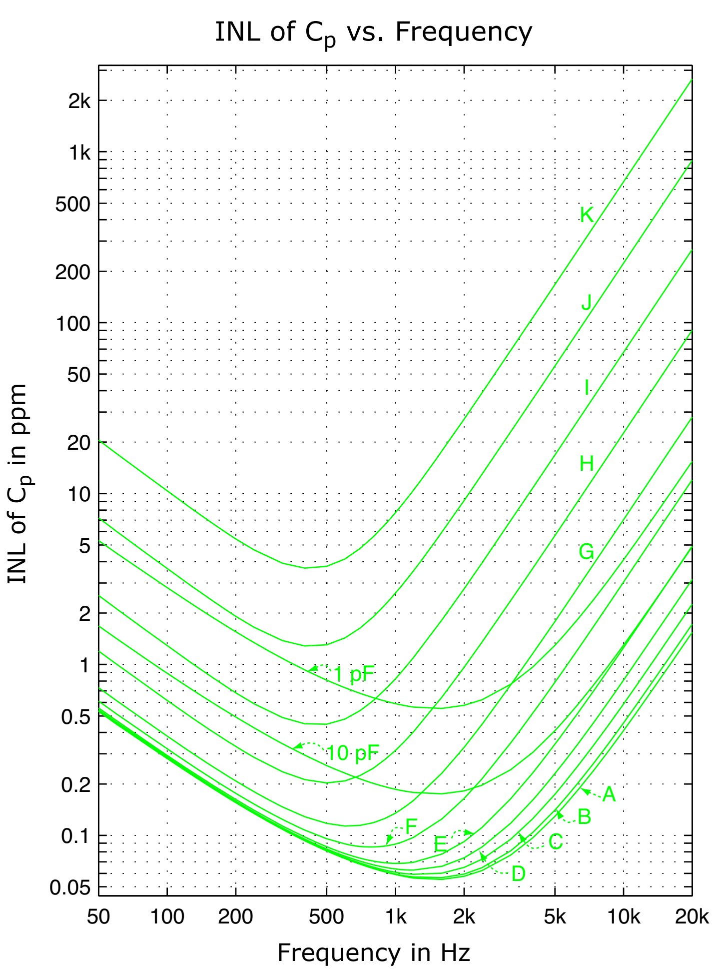

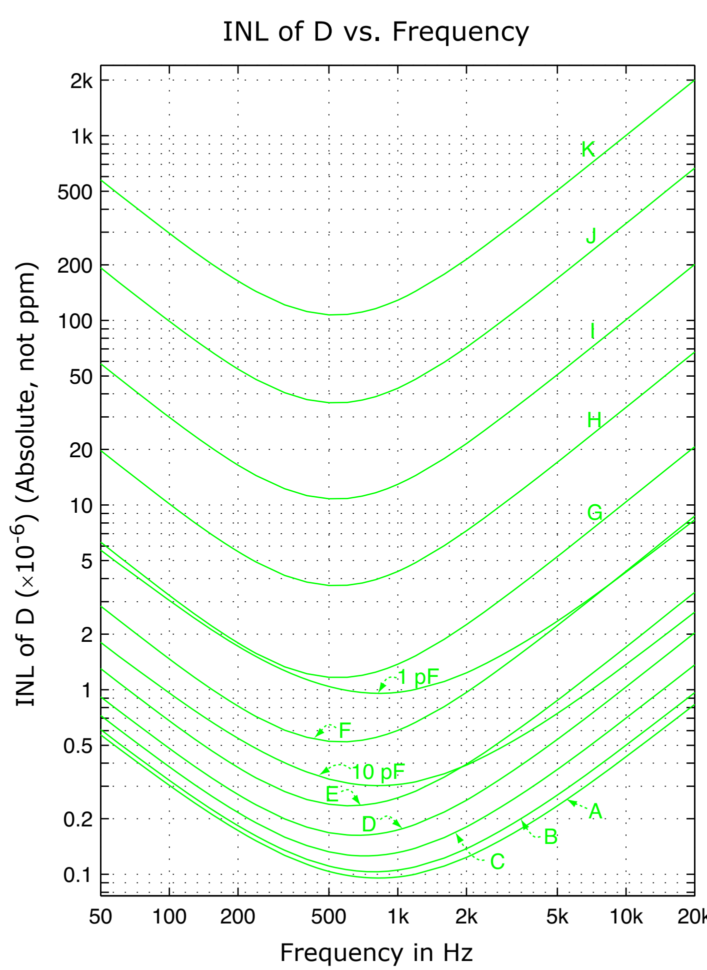

In contrast, each AH2700A Option-E bridge comes with a DCOAX-TPG-1-BNC one meter cable. This cable has double-braided silver plated shields and gold plated BNC connectors. This construction allows the cable's electrical parameters and its frequency dependent behavior to be more accurately and stably defined.

The AH2700A Option-E bridge introduces a new ability to select *correction models* for specific cable types and DUT configurations. These models have a built-in knowledge of electrical parameters for specific cable and DUT types. This includes the frequency dependence of these parameters if it's significant.

One of these models is for use with the DCOAX-TPG-1-BNC cable alone. Another is for use with that cable together with the AHTTA1 two-terminal to three-terminal adapter. These correction models are selectable by default as an alternative to the ability to specify individual cable electrical parameters for cable correction.

DUT Loading Corrections

Stray capacitance from high-to-ground (C_{HG}) and low-to-ground (C_{LG}) at the DUT causes the measured capacitance to be larger than it should by amounts that are proportional to C_{HG} and C_{LG}. Loading errors like these are discussed in NIST Special Publication 250-76. The AH2700A Option-E allows the user to enter the values for C_{HG} and C_{LG} at the DUT when using any of the correction models associated with the DCOAX-TPG-1-BNC cable. When using these models, the bridge will always automatically correct the measurement results for these stray capacitances. If C_{HG} and C_{LG} have never been entered, then default values will be used.

The Specification Equations

The specifications below give various performance uncertainties as a function mainly of capacitance, loss and frequency. See page 5 of the basic AH2700A brochure for definitions of all the input variables used. Other helpful relations are on page 4 herein.

Table 2. Capacitance and conductance ranges for the preferred limiting voltages with $f \geq 1$ kHz. For $f < 1$ kHz, multiply Limit by f in kHz. A_T, A_C and V_T are used by the specification equations.

Attenuator Tap	Limit (V_T)	Capacitance range	Range of G; f is in kHz	A_T	A_C
A	15.00 V	-11 to +110 pF	-0.8 f to +8 f nS	0	0
B	7.50 V	-22 to +220 pF	-1.6 f to +16 f nS	0	0
C	3.00 V	-55 to +550 pF	-4 f to +40 f nS	0	0
D	1.50 V	-110 to +1100 pF	-8 f to +80 f nS	0	0
E	0.750 V	-220 to +2200 pF	-16 f to +160 f nS	0	0
F	0.250 V	-660 to +6600 pF	-48 f to +480 f nS	0	0
G	0.100 V	-1650 to +16,500 pF	-120 f to +1200 f nS	5	0.01
H	0.030 V	-5500 to +55,000 pF	-400 f to +4000 f nS	10	0.03
I	0.010 V	-16,500 to +165,000 pF	-1200 f to +12,000 f nS	15	0.1
J	0.003 V	-55,000 to +550,000 pF	-4000 f to +40,000 f nS	20	0.3
K	0.001 V	-165,000 to +1650,000 pF	-12,000 f to +120,000 f nS	30	1

Accuracy in ppm following calibration:

Parallel:

$$C:\ \pm\left\{\frac{3}{10}\left[8+\frac{1}{f}+f\right]+\frac{1.5}{CV}\left[2+\frac{1}{3f}\right]+100D+\frac{f^2}{200}\left[1+\frac{1700}{200+CV}\right]+\frac{A_T}{10}\left[f^2+\frac{1}{f}\right]+3\times10^{-6}f^2C+\frac{f^2}{8C}\right\}$$

A_T is found in Table 2.

$$G:\ \pm\left\{100+\frac{\omega}{G}\left[\frac{C}{2}\left(1.2+\frac{1}{f}+f\right)+\frac{1.5}{V}\left(2+\frac{1}{3f}\right)+\frac{fC^2}{5000}+\frac{fC}{6}\left(1+\frac{1700}{200+CV}\right)+\frac{A_TC}{3}\left(f+\frac{1}{f}\right)\right]+\left\{\frac{\omega f}{G}\left[\frac{2\times10^{-4}}{3}C^2+\frac{f}{8}\right]\right\}\right\}$$

$$D:\ \pm\left\{\frac{(1+D^2)^{1/2}}{D}\left[100D+\frac{1}{2}\left(1.2+\frac{1}{f}+f\right)+\frac{1.5}{CV}\left(2+\frac{1}{3f}\right)+\frac{fC}{5000}+\frac{f}{6}\left(1+\frac{1700}{200+CV}\right)+\frac{A_T}{3}\left(f+\frac{1}{f}\right)\right]+\left\{\frac{(1+D^2)^{1/2}f}{D}\left[\frac{2\times10^{-4}}{3}C+\frac{f}{8C}\right]\right\}\right\}$$

$$R_P:\ \pm\left\{100+\omega R_p\left[\frac{C}{2}\left(1.2+\frac{1}{f}+f\right)+\frac{1.5}{V}\left(2+\frac{1}{3f}\right)+\frac{fC^2}{5000}+\frac{fC}{6}\left(1+\frac{1700}{200+CV}\right)+\frac{A_TC}{3}\left(f+\frac{1}{f}\right)\right]+\left\{\omega R_p f\left[\frac{2\times10^{-4}}{3}C^2+\frac{f}{8}\right]\right\}\right\}$$

Series:

$$C_S:\ \pm\left\{\frac{3}{10}\left[8+\frac{1}{f}+f\right]+\frac{1.5}{C_sV}\left[2+\frac{1}{3f}\right](1+D^2)+100D+\frac{f^2}{200}\left[1+\frac{1700}{200+CV}\right]+\frac{A_T}{10}\left[f^2+\frac{1}{f}\right]+3\times10^{-6}f^2C+\frac{f^2(1+D^2)}{8C_s}\right\}$$

$$R_S:\ \pm\left\{100+\frac{50}{R_s}+\frac{1}{D}\left[\frac{1}{2}\left(1.2+\frac{1}{f}+f\right)+\frac{1.5}{C_sV}\left(2+\frac{1}{3f}\right)(1+D^2)+\frac{f}{6}\left(1+\frac{1700}{200+CV}\right)+\frac{A_T}{3}\left(f+\frac{1}{f}\right)\right]+\left\{\frac{30}{R_s}+\frac{f^2(1+D^2)}{8DC_s}\right\}\right\}$$

The length of the cables connecting the 2700A to the DUT has a negligible effect on the accuracy for *small* capacitances. This assumes that the coaxial shield on these cables has 100% coverage. If uncorrected by the CABLE command, cables similar to RG-58 will increase the capacitance readings at 1kHz by about 40 ppm per meter of cable pair and per µF of capacitance being measured.

The accuracy Y years following calibration may be calculated from the expression A + YS where A is the desired accuracy expression from above and S is the corresponding stability per year below.

Resolution in absolute units:*

Parallel:

$$C: \left\{\frac{C}{40}\left[2+\frac{1}{f}\right]+\frac{1.5}{V}\left[2+\frac{1}{3f}+5n_c\right]+\frac{n_vC}{V}+\frac{20G}{\omega}+(1+10A_C)\frac{f^2C}{1000}\left[1+\frac{1700}{200+CV}\right]\right\}\times 10^{-6}\ \text{pF}$$

$$G: \left\{20G+\omega\left[\frac{C}{40}\left(2+\frac{1}{f}\right)+\frac{1.5}{V}\left(2+\frac{1}{3f}+5n_c\right)+\frac{n_vC}{V}+8\times10^{-6}fC^2+(3+50A_C)\frac{fC}{100}\left(1+\frac{1700}{200+CV}\right)\right]\right\}\times 10^{-6}\ \text{nS}$$

Divide result by ω to get absolute resolution for G/ω

$$D: \left\{\sqrt{1+D^2}\left[20D+\frac{1}{40}\left(2+\frac{1}{f}\right)+\frac{1.5}{CV}\left(2+\frac{1}{3f}+5n_c\right)+\frac{n_v}{V}+8\times10^{-6}fC+(3+50A_C)\frac{f}{100}\left(1+\frac{1700}{200+CV}\right)\right]\right\}\times 10^{-6}$$

$$R_P: \left\{20R_p+\omega R_p^2\left[\frac{C}{40}\left(2+\frac{1}{f}\right)+\frac{1.5}{V}\left(2+\frac{1}{3f}+5n_c\right)+\frac{n_vC}{V}+8\times10^{-6}fC^2+(3+50A_C)\frac{fC}{100}\left(1+\frac{1700}{200+CV}\right)\right]\right\}\times 10^{-6}\ \text{G}\Omega$$

Series:

$$C_S: \left\{\frac{C_s}{40}\left[2+\frac{1}{f}\right]+\frac{1.5}{V}\left[2+\frac{1}{3f}+5n_c\right](1+D^2)+\frac{n_vC_s}{V}+20DC_s+(1+10A_C)\frac{f^2C_s}{1000}\left[1+\frac{1700}{200+CV}\right]\right\}\times 10^{-6}\ \text{pF}$$

$$R_S: \left\{20R_s+1.3+\frac{R_s}{D}\left[\frac{1}{40}\left(2+\frac{1}{f}\right)+\frac{1.5}{C_sV}\left(2+\frac{1}{3f}+5n_c\right)(1+D^2)+\frac{n_v}{V}+(3+50A_C)\frac{f}{100}\left(1+\frac{1700}{200+CV}\right)\right]\right\}\times 10^{-6}\ \text{k}\Omega$$

where $n_c = 1.4t^{-1/2}$ and $n_v = 0.01(1+0.1/f)(R_S+10)^{1/2}(1+D^2)^{1/2}t^{-1/2}$. A_C is found in Table 2.
The series resistance R_S needed for n_v may be calculated using $R_S = D\times10^6/(\omega C(1+D^2))$.

Resolution in ppm:*

Parallel:

$$C: \frac{1}{40}\left[2+\frac{1}{f}\right]+\frac{1.5}{CV}\left[2+\frac{1}{3f}+5n_c\right]+\frac{n_v}{V}+20D+(1+10A_C)\frac{f^2}{1000}\left[1+\frac{1700}{200+CV}\right]$$

$$G: 20+\frac{\omega}{G}\left\{\frac{C}{40}\left[2+\frac{1}{f}\right]+\frac{1.5}{V}\left[2+\frac{1}{3f}+5n_c\right]+\frac{n_vC}{V}+8\times10^{-6}fC^2+(3+50A_C)\frac{fC}{100}\left[1+\frac{1700}{200+CV}\right]\right\}$$

$$D: \frac{(1+D^2)^{1/2}}{D}\left\{20D+\frac{1}{40}\left[2+\frac{1}{f}\right]+\frac{1.5}{CV}\left[2+\frac{1}{3f}+5n_c\right]+\frac{n_v}{V}+8\times10^{-6}fC+(3+50A_C)\frac{f}{100}\left[1+\frac{1700}{200+CV}\right]\right\}$$

$$R_P: 20+\omega R_p\left\{\frac{C}{40}\left[2+\frac{1}{f}\right]+\frac{1.5}{V}\left[2+\frac{1}{3f}+5n_c\right]+\frac{n_vC}{V}+8\times10^{-6}fC^2+(3+50A_C)\frac{fC}{100}\left[1+\frac{1700}{200+CV}\right]\right\}$$

Series:

$$C_S: \frac{1}{40}\left[2+\frac{1}{f}\right]+\frac{1.5}{C_sV}\left[2+\frac{1}{3f}+5n_c\right](1+D^2)+\frac{n_v}{V}+20D+(1+10A_C)\frac{f^2}{1000}\left[1+\frac{1700}{200+CV}\right]$$

$$R_S: 20+\frac{1.3}{R_s}+\frac{1}{D}\left\{\frac{1}{40}\left[2+\frac{1}{f}\right]+\frac{1.5}{C_sV}\left[2+\frac{1}{3f}+5n_c\right](1+D^2)+\frac{n_v}{V}+(3+50A_C)\frac{f}{100}\left[1+\frac{1700}{200+CV}\right]\right\}$$

*Resolution is the smallest *repeatable* difference in readings that is *guaranteed* to be measurable at *every* capacitance or loss value.
Useful resolution is typically a factor of ten better.

Input Noise:

Parallel:

$$C: \frac{1}{CV}\left\{\frac{1.3}{f}+0.023(C\sqrt{1+D^2}+600)\left[\frac{R_sC^2}{2(C+300)^2}+1\right]^{1/2}\right\}/\sqrt{Hz}$$

$$G: \frac{\omega}{CV}\left\{\frac{1.3}{f}+0.023(C\sqrt{1+D^2}+600)\left[\frac{R_sC^2}{2(C+300)^2}+1\right]^{1/2}\right\}/\sqrt{Hz}$$

$$D: \frac{1}{CV\sqrt{1+D^2}}\left\{\frac{1.3}{f}+0.023(C\sqrt{1+D^2}+600)\left[\frac{R_sC^2}{2(C+300)^2}+1\right]^{1/2}\right\}/\sqrt{Hz}$$

$$R_P: \frac{\omega R_p}{V}\left\{\frac{1.3}{f}+0.023(C\sqrt{1+D^2}+600)\left[\frac{R_sC^2}{2(C+300)^2}+1\right]^{1/2}\right\}/\sqrt{Hz}$$

Series:

$$C_S: \frac{1+D^2}{C_sV}\left(\frac{1.3}{f}+0.023\left(\frac{C_s}{\sqrt{1+D^2}}+600\right)\left[\frac{R_sC^2}{2(C+300)^2}+1\right]^{1/2}\right)/\sqrt{Hz}$$

$$R_S: \frac{1+D^2}{DV}\left(\frac{1.3}{fC_s}+0.023\left(\frac{1}{\sqrt{1+D^2}}+\frac{600}{C_s}\right)\left[\frac{R_sC^2}{2(C+300)^2}+1\right]^{1/2}\right)/\sqrt{Hz}$$

Useful Unit Conversions

The relationships below can be useful for converting from one kind of units to another. Particularly useful are conversions from other units to the units of C or G for use in Table 2 on page 3.

$$G = \omega CD = 1/R_p$$

$$D = \omega C_sR_s10^{-6} = 1/(\omega CR_p)$$

$$C = C_s/(1+\omega^2C_s^2R_s^210^{-12})$$

$$G = 10^6/[R_s+10^{12}/(\omega^2C_s^2R_s)]$$

Accuracy of C_p vs. Frequency

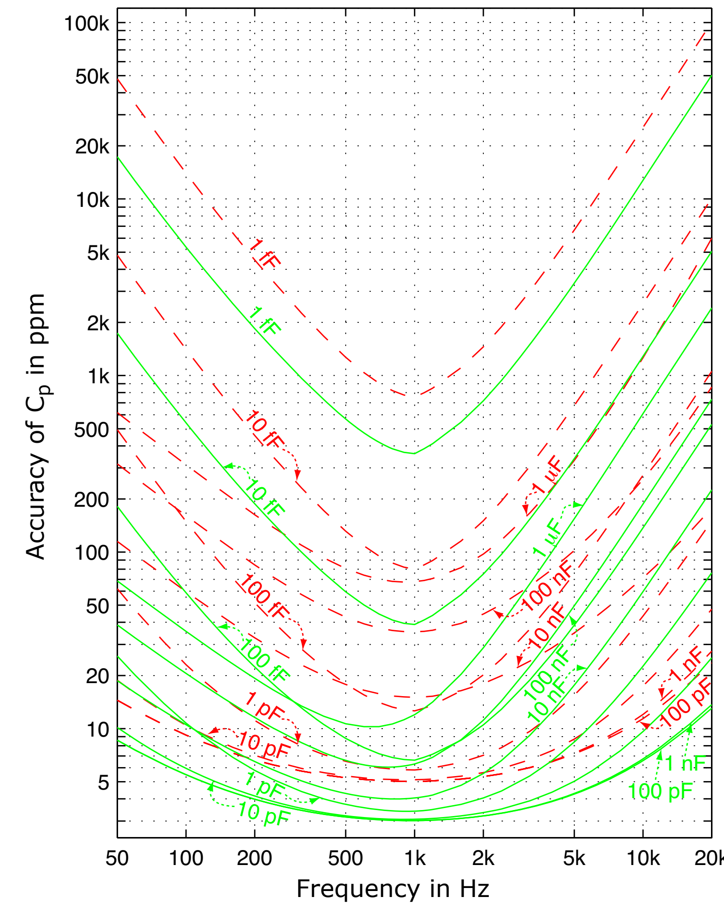

Accuracy of D vs. Frequency

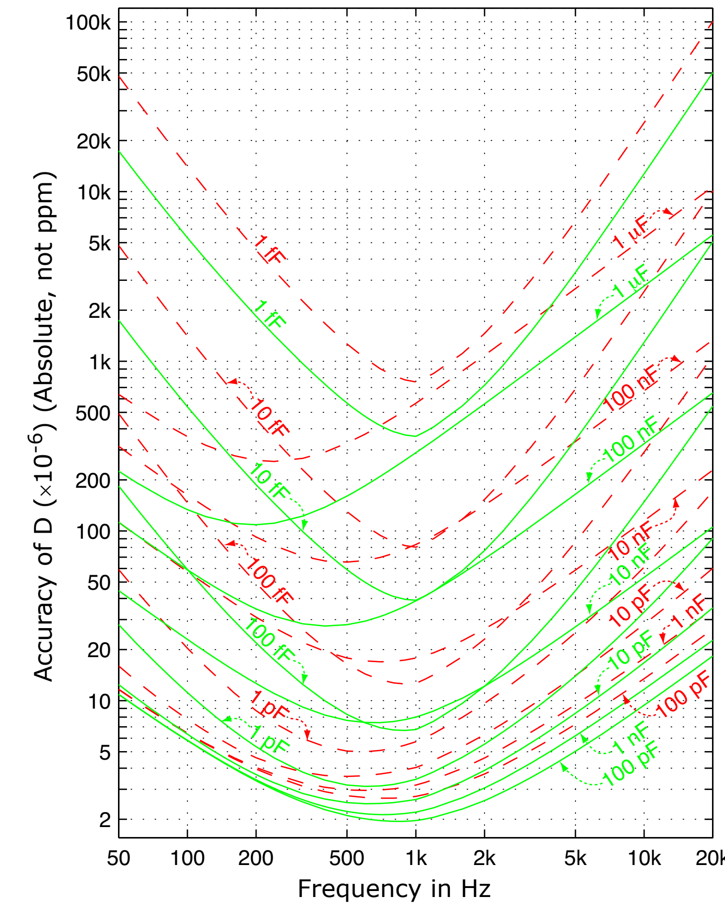

Stability/Year of C_p vs. Frequency

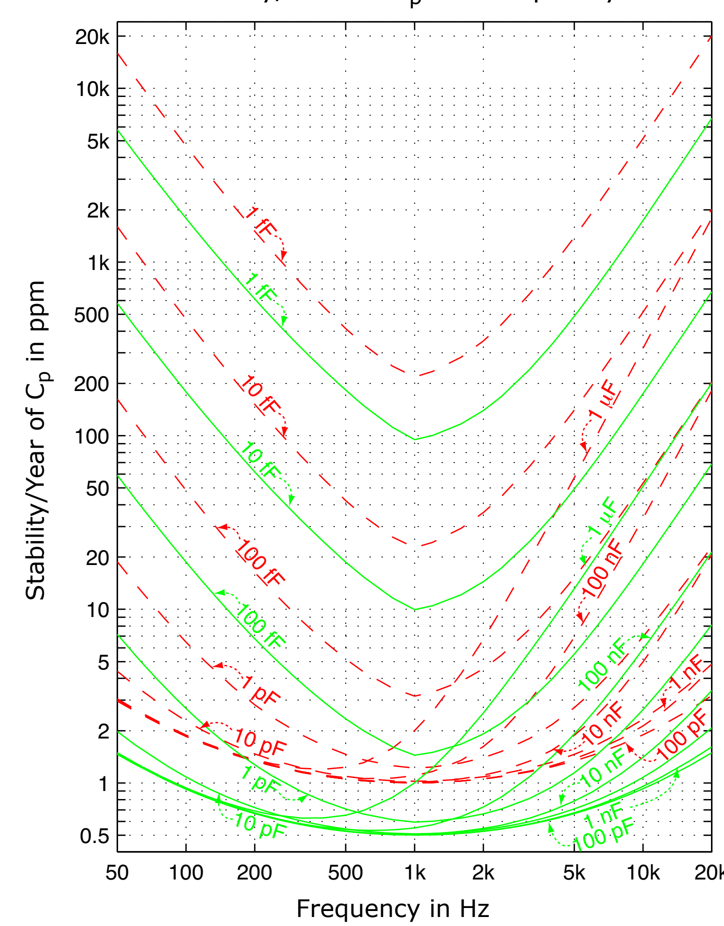

Stability/Year of D vs. Frequency

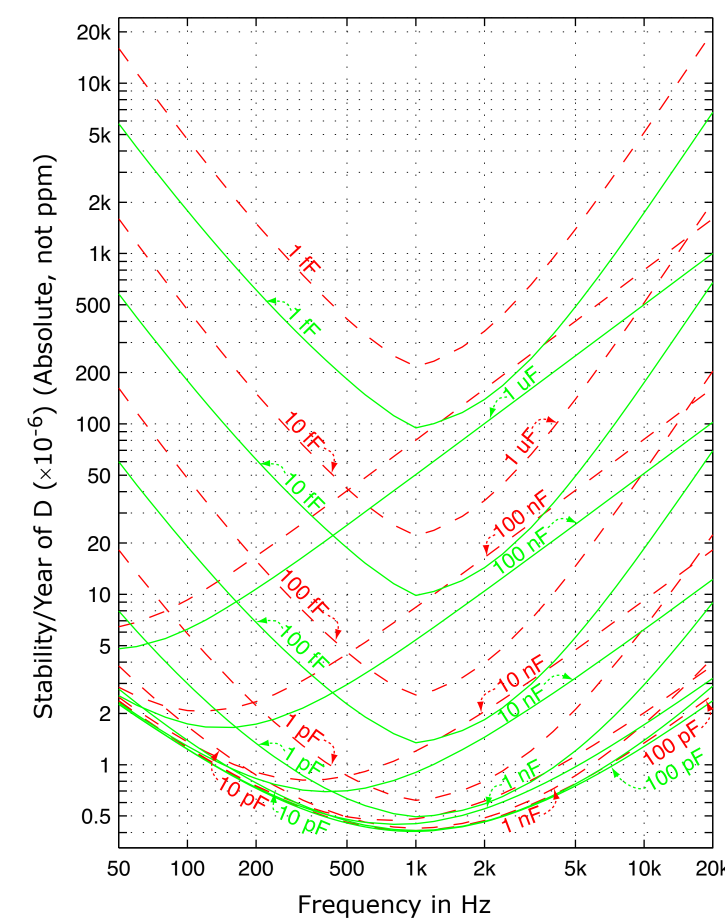

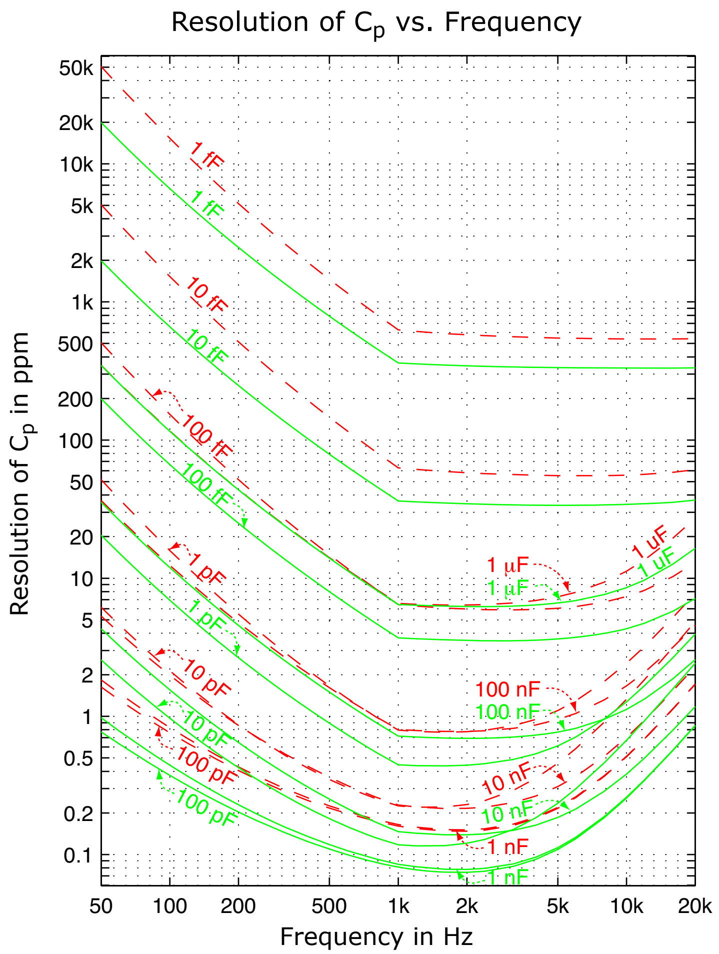

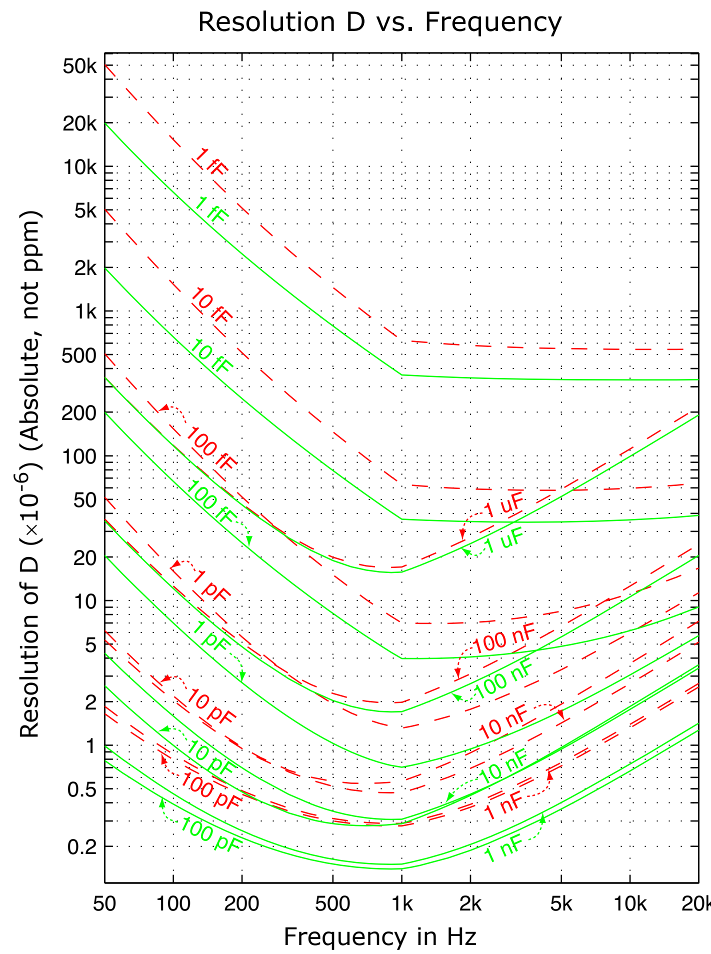

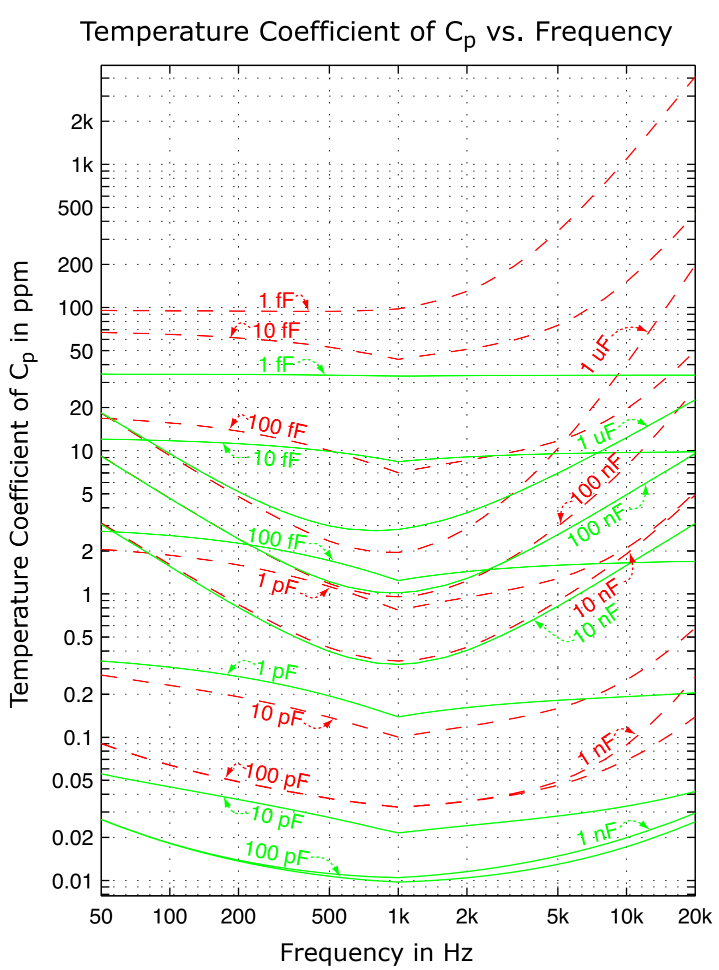

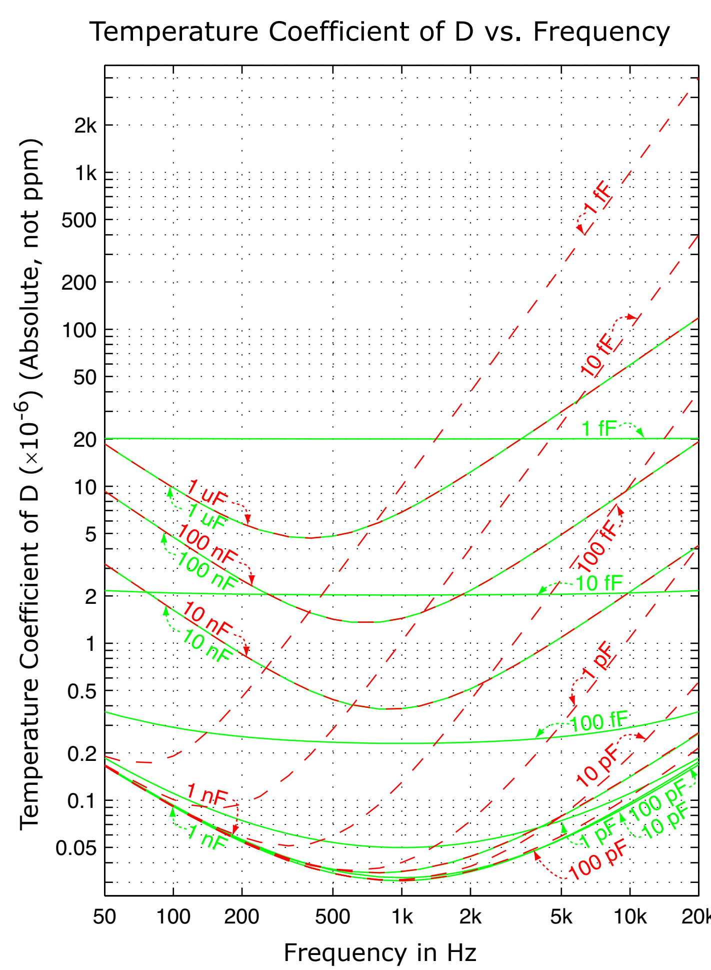

Attenuator Pair Ratio (APR) Uncertainty in ppm:

As discussed in more detail on page 2, the APR specification gives the additional uncertainty between a pair of measurements made using two different attenuator taps, T_1 and T_2. These can have values from A to K. For a given pair of taps, the values of V_1, V_2, A_{T_1} and A_{T_2} can be found in Table 2 on page 3. All usable pairs of taps are plotted in graphs on pages 11 & 12.

Parallel:

$$C: \pm\left\{\left|log_{10}\left(\frac{V_1}{V_2}\right)\right|\left(0.15 + \frac{0.12}{f} + 0.03f^2\right) + \frac{1}{20000}\left(90 + \frac{4}{f} + 10f^2\right)\left|\frac{1}{V_1} - \frac{1}{V_2}\right| + \frac{0.1}{f}\left|A_{T_1} - A_{T_2}\right|\right\}$$

$$G: \pm\frac{1}{D}\left\{\left|log_{10}\left(\frac{V_1}{V_2}\right)\right|\left(0.12 + \frac{0.12}{f} + 0.06f\right) + \frac{1}{1000}\left(5 + \frac{2}{f} + f\right)\left|\frac{1}{V_1} - \frac{1}{V_2}\right| + \frac{0.1}{f}\left|A_{T_1} - A_{T_2}\right|\right\}$$

$$D: \pm\left\{\left|log_{10}\left(\frac{V_1}{V_2}\right)\right|\left(0.12 + \frac{0.12}{f} + 0.06f\right) + \frac{1}{1000}\left(5 + \frac{2}{f} + f\right)\left|\frac{1}{V_1} - \frac{1}{V_2}\right| + \frac{0.1}{f}\left|A_{T_1} - A_{T_2}\right|\right\}$$

$$R_P: \pm\frac{1}{D}\left\{\left|log_{10}\left(\frac{V_1}{V_2}\right)\right|\left(0.12 + \frac{0.12}{f} + 0.06f\right) + \frac{1}{1000}\left(5 + \frac{2}{f} + f\right)\left|\frac{1}{V_1} - \frac{1}{V_2}\right| + \frac{0.1}{f}\left|A_{T_1} - A_{T_2}\right|\right\}$$

Series:

$$C_S: \pm\left\{\left|log_{10}\left(\frac{V_1}{V_2}\right)\right|\left(0.15 + \frac{0.12}{f} + 0.03f^2\right) + \frac{1}{20000}\left(90 + \frac{4}{f} + 10f^2\right)\left|\frac{1}{V_1} - \frac{1}{V_2}\right| + \frac{0.1}{f}\left|A_{T_1} - A_{T_2}\right|\right\}$$

$$R_S: \pm\frac{1}{D}\left\{\left|log_{10}\left(\frac{V_1}{V_2}\right)\right|\left(0.12 + \frac{0.12}{f} + 0.06f\right) + \frac{1}{1000}\left(5 + \frac{2}{f} + f\right)\left|\frac{1}{V_1} - \frac{1}{V_2}\right| + \frac{0.1}{f}\left|A_{T_1} - A_{T_2}\right|\right\}$$

Differential Non-Linearity (DNL) in ppm:

This DNL specification assumes that the DDNL correction feature is disabled. Enabling DDNL can often improve DNL substantially. The feature's effect is to reduce the mathematical derivative of the measurement results as a function of capacitance or loss.

Parallel:

$$C: \pm\left\{\frac{1}{40}\left(2 + \frac{1}{f}\right) + 20D + \frac{f^2}{500}\left[\frac{300 + 2000(1 - e^{-1.5/V})}{100 + CV}\right] + \frac{3 + 0.6\,log_{10}CV}{CV}\right\}$$

$$G: \pm\left\{20 + \frac{\omega}{G}\left[\frac{C}{40}\left(2 + \frac{1}{f}\right) + \frac{fC}{50}\left[\frac{1200 + 1500(1 - e^{-1.5/V})}{100 + CV}\right] + \frac{3 + 0.6\,log_{10}CV}{CV}\right]\right\}$$

$$D: \pm\left\{\frac{\sqrt{1 + D^2}}{D}\left[20D + \frac{1}{40}\left(2 + \frac{1}{f}\right) + \frac{f}{50}\left[\frac{1200 + 1500(1 - e^{-1.5/V})}{100 + CV}\right] + \frac{3 + 0.6\,log_{10}CV}{CV}\right]\right\}$$

$$R_P: \pm\left\{20 + \omega R_P\left[\frac{C}{40}\left(2 + \frac{1}{f}\right) + \frac{fC}{50}\left[\frac{1200 + 1500(1 - e^{-1.5/V})}{100 + CV}\right] + \frac{3 + 0.6\,log_{10}CV}{CV}\right]\right\}$$

Series:

$$C_S: \pm\left\{\frac{1}{40}\left(2 + \frac{1}{f}\right) + 20D + \frac{f^2}{500}\left[\frac{300 + 2000(1 - e^{-1.5/V})}{100 + CV}\right] + \frac{3 + 0.6\,log_{10}CV}{CV}\right\}$$

$$R_S: \pm\left\{20 + \frac{1}{D}\left[\frac{1}{40}\left(2 + \frac{1}{f}\right) + \frac{f}{50}\left[\frac{1200 + 1500(1 - e^{-1.5/V})}{100 + CV}\right] + \frac{3 + 0.6\,log_{10}CV}{CV}\right]\right\}$$

Integral Non-Linearity (INL) in ppm:

Parallel:

$$C: \pm\left\{0.03 + \frac{1}{40f} + \frac{f^2}{300} + \frac{1}{V_T}\left[\frac{1}{1000f} + \frac{f^2}{150}\right]\right\}$$

$$G: \pm\frac{1}{D}\left\{0.03 + \frac{1}{40f} + \frac{f}{30} + \frac{1}{V_T}\left[\frac{1}{35f} + \frac{f}{10}\right]\right\}$$

$$D: \pm\left\{0.03 + \frac{1}{40f} + \frac{f}{30} + \frac{1}{V_T}\left[\frac{1}{35f} + \frac{f}{10}\right]\right\}$$

$$R_P: \pm\frac{1}{D}\left\{0.03 + \frac{1}{40f} + \frac{f}{30} + \frac{1}{V_T}\left[\frac{1}{35f} + \frac{f}{10}\right]\right\}$$

Series:

$$C_S: \pm\left\{0.03 + \frac{1}{40f} + \frac{f^2}{300} + \frac{1}{V_T}\left[\frac{1}{1000f} + \frac{f^2}{150}\right]\right\}$$

$$R_S: \pm\frac{1}{D}\left\{0.03 + \frac{1}{40f} + \frac{f}{30} + \frac{1}{V_T}\left[\frac{1}{35f} + \frac{f}{10}\right]\right\}$$

$$C: \pm\frac{10}{\sqrt{C_{max}}}\left\{0.03 + \frac{1}{40f} + \frac{f^2}{300} + \frac{1}{15}\left[\frac{1}{1000f} + \frac{f^2}{150}\right]\right\}$$

$$G: \pm\frac{10}{D\sqrt{C_{max}}}\left\{0.03 + \frac{1}{40f} + \frac{f}{30} + \frac{1}{15}\left[\frac{1}{35(700)f} + \frac{f}{10}\right]\right\}$$

The six equations to the left give the INL uncertainty for each attenuator tap. These range from A to K and are listed in Table 2 on page 3. The value of V_T is given there also.

The two equations above give the INL uncertainty for smaller capacitance ranges bounded by 0.0 and C_{max} where C_{max} can have values of 1.0 and 10.0 pF.

This INL uncertainty specifies the maximum difference of the sum of the capacitances of two capacitors measured individually against measurements of them taken when connected in parallel. This specification is valid only if all three measurements are taken using the same attenuator tap.

Stability in ppm per year:

Parallel:

$$C:\ \pm\left\{\frac{1}{20}\left[8+\frac{1}{f}+f\right]+\frac{1}{2CV}\left[2+\frac{1}{3f}\right]+20D+5\times10^{-7}f^2C+\frac{f^2}{60C}\right\}$$

$$G:\ \pm\left\{20+\frac{\omega}{G}\left[\frac{C}{10}\left(2+\frac{1}{f}+f\right)+\frac{1}{2V}\left(2+\frac{1}{3f}\right)+3\times10^{-5}fC^2\right]+\frac{\omega f}{G}\left[2\times10^{-5}C^2+\frac{f}{60}\right]\right\}$$

$$D:\ \pm\left\{\frac{(1+D^2)^{1/2}}{D}\left[20D+\frac{1}{10}\left(2+\frac{1}{f}+f\right)+\frac{1}{2CV}\left(2+\frac{1}{3f}\right)+3\times10^{-5}fC\right]+\frac{(1+D^2)^{1/2}f}{D}\left[2\times10^{-5}C+\frac{f}{60C}\right]\right\}$$

$$R_P:\ \pm\left\{20+\omega R_p\left[\frac{C}{10}\left(2+\frac{1}{f}+f\right)+\frac{1}{2V}\left(2+\frac{1}{3f}\right)+3\times10^{-5}fC^2\right]+\omega R_p f\left[2\times10^{-5}C^2+\frac{f}{60}\right]\right\}$$

Series:

$$C_S:\ \pm\left\{\frac{1}{20}\left[8+\frac{1}{f}+f\right]+\frac{1}{2C_sV}\left[2+\frac{1}{3f}\right](1+D^2)+20D+5\times10^{-7}f^2C+\frac{f^2(1+D^2)}{60C_s}\right\}$$

$$R_S:\ \pm\left\{20+\frac{8}{R_s}+\frac{1}{D}\left[\frac{1}{10}\left(2+\frac{1}{f}+f\right)+\frac{1}{2C_sV}\left(2+\frac{1}{3f}\right)(1+D^2)\right]+\left\{\frac{5}{R_s}+\frac{f^2(1+D^2)}{60DC_s}\right\}\right\}$$

Temperature coefficient relative to change in ambient temperature in ppm per °C:

Parallel:

$$C:\ \pm\left\{\frac{1}{1200}\left[8+\frac{1}{f}+f\right]+10D+\frac{A_T}{33}\left[f+\frac{1}{f}\right]+\frac{30}{2+6CV(2+1/f)}+10^{-6}f^{1/2}C+\frac{1}{50C}\right\}$$

where A_T is found in Table 2.

$$G:\ \pm\left\{10+\frac{\omega C}{G}\left[\frac{3}{400}\left(2+\frac{1}{f}+f\right)+3\times10^{-6}fC+\frac{A_T}{33}\left(f+\frac{1}{f}\right)\right]+\frac{60}{4+VG(2+1/f)/\omega}+\frac{\omega C}{G}\left[2\times10^{-6}fC+\frac{1}{50C}\right]\right\}$$

$$D:\ \pm\left\{\frac{(1+D^2)^{1/2}}{D}\left[10D+\frac{3}{400}\left(2+\frac{1}{f}+f\right)+3\times10^{-6}fC+\frac{A_T}{33}\left(f+\frac{1}{f}\right)\right]+\frac{30}{2+6CV(2+1/f)}+\frac{60}{4+CVD(2+1/f)}+\frac{(1+D^2)^{1/2}f}{D}\left[2\times10^{-6}C+\frac{1}{50fC}\right]\right\}$$

$$R_P:\ \pm\left\{10+\omega CR_p\left[\frac{3}{400}\left(2+\frac{1}{f}+f\right)+3\times10^{-6}fC+\frac{A_T}{33}\left(f+\frac{1}{f}\right)\right]+\frac{60}{4+VG(2+1/f)/\omega R_p}+\omega CR_p\left[2\times10^{-6}fC+\frac{1}{50C}\right]\right\}$$

Series:

$$C_S:\ \pm\left\{\frac{1}{1200}\left[8+\frac{1}{f}+f\right]+10D+\frac{A_T}{33}\left[f+\frac{1}{f}\right]+\frac{30}{2+6C_sV(2+1/f)/(1+D^2)}+10^{-6}f^{1/2}C+\frac{1+D^2}{50C_s}\right\}$$

$$R_S:\ \pm\left\{10+\frac{0.5}{R_s}+\frac{1}{D}\left[\frac{3}{400}\left(2+\frac{1}{f}+f\right)+\frac{A_T}{33}\left(f+\frac{1}{f}\right)\right]+\frac{60}{4+6C_sV(2+1/f)/(1+D^2)}+\frac{0.3}{R_s}+\frac{1+D^2}{50C_s}\right\}$$

SELECTED SPECIFICATIONS IN GRAPHICAL FORM

Accuracy specifications versus C and loss

There are six contour plots on the next page. The first three graphs are contour plots of the accuracy of capacitance (C) versus C and conductance (G). The first of these graphs applies at 100 Hz, the second one at 1 kHz and the third one at 10 kHz. The accuracy in the area within or below each contour is equal to or better than the labeled accuracy (in percent) for that contour. These graphs show that the accuracy of C depends not only on the value of C but also on the value of the loss. Each contour was plotted using the maximum possible voltage.

The graph in the middle of the right column is a contour plot of the accuracy of the dissipation factor (D) versus C and D. The accuracy in the area within each contour is equal to or better than the labeled accuracy (in percent) for that contour. This graph shows that the accuracy of D depends not only on the value of D but also on the value of C.

Accuracy specifications at selected voltages

The first graph in the bottom row on the next page is a contour plot of the accuracy of C versus C and G. The accuracy in the area within or below each contour is equal to or better than 0.001%.

The second graph in the bottom row on the next page is a contour plot of the accuracy of D versus C and D. The accuracy in the area within each contour is equal to or better than 0.03%.

These graphs show how the accuracy of C and D depends on the measurement voltage. Each contour represents operation at the labeled voltage which is one of the voltages in Table 2 on page 3. The gray regions are out of range.

Option-E Specs Compared to non-Option-E

Selected specifications for both the AH2700A Option-E and non-Option-E are shown in the graphs below. Specifications for the non-Option-E AH2700A are shown in red while specifications for the Option-E are shown in green.

Specifications versus frequency

There are 16 graphs on pages 8-12 of plots versus frequency for capacitance and loss. These include the accuracy, resolution in ppm, temperature coefficient, accuracy, stability, DNL, INL, input noise, and APR specifications. These plots were generated by using the specification equations presented on pages 3-6. The exception is that the equations for D are multiplied by D to get units of absolute D. Most graphs contain a set of curves for various values of capacitance. These values range from one femtoFarad up to one microFarad. The graphs show that the specifications tend to be best for capacitance values in the region of 10 pF to 1 nF and worst at either extreme of capacitance. These graphs assume that the capacitance of the DUT is of good quality implying a small dissipation factor (D<~0.001). Most curves were plotted using the maximum possible voltage.